Towards observation of sub-diffractive pulse propagation in photonic crystals

Yu. Loiko [a,b], K. Staliunas [a,c,*], R. Herrero [a], C. Cojocaru [a], J. Trull [a],
V. Sirutkaitis [d], D. Faccio [e], T. Pertsch [f]

[a] *Departament de Física i Enginyeria Nuclear, Universitat Politècnica de Catalunya, Colom 11, 08222 Terrassa, Spain*
[b] *Institute of Molecular and Atomic Physics, National Academy of Sciences of Belarus, Nezaleznasty Avenue 70, 220072 Minsk, Belarus*
[c] *Institució Catalana de Reserca i Estudis Avançats (ICREA), E-08010 Barcelona, Spain*
[d] *Laser Research Centre, Vilnius University, Sauletekio al. 10, LT-10222 Vilnius, Lithuania*
[e] *Dipartimento di Fisica e Matematica, Università dell'Insubria, Via Valleggio 11, 22100 Como, Italy*
[f] *Friedrich-Schiller-Universität Jena, Institut für Angewandte Physik, Max-Wien-Platz 1, D-07743 Jena, Germany*

Abstract

It is shown that sub-diffractive (self-collimating) propagation of ultrashort pulses of narrow light beams is possible in two dimensional planar photonic crystal slabs (in particular made with air holes in Si_3N_4 slab) where the sub-diffractive propagation of monochromatic beam of visible light has been demonstrated previously both theoretically and numerically. We found that the sub-diffractive propagations of the pulses of duration of more than 40 fs are indistinguishable from that of monochromatic beams. However, for the pulses with duration less than 40 fs their propagation peculiarities associated with asymmetric spatiotemporal misshaping, spatial and temporal broadening come into play. The effects are pronounced for the pulses of duration less than 20 fs. The phenomena are shown for both TM and TE polarized light by means of numerical integration of 2D Maxwell's equations with finite-difference time-domain technique.
© 2007 Elsevier B.V. All rights reserved.

1. Introduction

It is well known that the diffraction of light beams becomes strong when the beam diameter approaches the light wavelength limit [1]. Therefore, the management and control of light diffraction is an important problem in developing of micro- and nano-meter scale optoelectronic circuits. Recently, it has been shown [2–19] that the management of light diffraction can be provided by making a photonic crystal (PC) structure inside a medium which light passed through. Propagation of stationary light beams without substantial spreading in transverse direction on a distance much longer than the Rayleigh length has

been demonstrated experimentally [2–10] and investigated in details theoretically in PCs with steeped [11–15] and harmonic [16–19] spatial modulation of the refractive index. Such regimes of non-spreading light propagation have been called self-collimation or sub-diffractive ones. In particular it has been shown that the sub-diffractive propagation for monochromatic waves occurs at a fixed frequency for a given set of the PC's parameters called as zero diffraction point (ZDP) [17,18].

Since, the light pulses could be used for transfer and processing the data in the integrated micro-optoelectronic circuits, there is an interest on the investigation of diffraction management of pulsed light beams. Promising candidate for this purpose could be the PCs mentioned above under the conditions when stationary light beams propagate sub-diffractively. However, since the pulse contains different spectral components, the diffraction can not vanish for all frequencies simultaneously. Particularly, if the central

---

* Corresponding author. Address: Departament de Física i Enginyeria Nuclear, Universitat Politècnica de Catalunya, Colom 11, 08222 Terrassa, Spain.
  E-mail address: kestutis.staliunas@icrea.es (K. Staliunas).

frequency component of a pulse is tuned to the ZDP, then the lower and the higher frequency components will propagate with the normal and anomalous diffraction, respectively. Consequently, the ultrashort and ultranarrow pulses misshape during the propagation in such PCs, and, in overall, they should diffract more than the corresponding monochromatic beam in sub-diffractive PCs under the same conditions. This phenomenon has been predicted and studied for the first time in Ref. [19] in PC with harmonic modulation of the refractive index profile and under paraxial approximation. Since, the main part of PCs available on the market is made with steeped profile of refractive index, for instance, with air holes in homogeneous materials, the previously obtained results are only strictly applicable for such structures.

Therefore, in this paper we are aimed (i) to provide theoretical investigations on the pulsed light beam propagation in the PCs in which sub-diffractive propagation of stationary beams takes place, (ii) to show that strong reduction of the transverse spreading of the pulsed light beams is possible in such PCs, and (iii) to justify the conditions and extend analytical results for sub-diffractive propagation of pulsed light beams beyond the paraxial approximation and for PCs with steeped profile of the refractive index modulation.

For these purposes we simulate by finite-difference time-domain (FDTD) method the pulse propagation in a planar two dimensional (2D) PC in which the sub-diffractive light propagation of monochromatic beams has been observed previously in experiments for visible light [8]. The main parameters of the investigated PC and the full sets of Maxwell's equations for TE and TM polarized light are introduced in Section 2. In Section 3 we give analytical estimation for characteristic lengths that describe the effect of different mechanisms on the pulse spreading in considered 2D planar PCs and compare spreading of TE and TM polarized pulses in PCs with their spreading in homogeneous medium. Because the pulse width and the carrier frequency of the pulse are the main variable parameters in the experiments, in Section 4 we investigate how these parameters affect the light pulse propagation and we show numerically that strong reduction of pulsed light spreading in the considered PCs is possible under appropriate conditions for both TE and TM polarizations. We plot typical spatio-temporal distributions of the radiation in the pulsed beams, and we calculate the evolution of the width and the duration of the pulses during the propagation. We also investigate the dependence of the pulse characteristics on the central frequency of the radiation. In order to optimize the design of the samples for future possible experiments, we vary the propagation constant of the planar waveguide mode, which corresponds to a change in the thickness of the sample. In Section 5 we summarize obtained results.

2. Model

We consider a planar (2D) PCs that consists of a waveguide slab on the top of which a lattice of air holes is etched. The refractive indexes of the top and bottom cladding layers are smaller than that of the core layer in order to obtain the confinement of the light modes in vertical direction. Previously, it has been shown [8,11,12] that light propagation in such planar PCs could be described by considering the effective refractive index of the PC material, which corresponds only to a particular propagation mode of the waveguide. We will follow this direction, i.e. we consider propagation of pulsed light beams in two spatial dimensions of 2D PCs with a lattice of holes that takes the same form as in the real PC, but we consider effective index of refraction for the bulk material, in which the holes are made, on the basis of calculation of propagation vector of the guided modes formed in the real PC. Our waveguide consists of a 250 nm thick Si_3N_4 layer with a top and a bottom layer of SiO_2. Previously, it has been shown that using this $SiO_2/Si_3N_4/SiO_2$ waveguide configuration the sub-diffractive propagation of stationary light beams is possible near the wavelength $\lambda_0 = 800$ nm for the following parameters of the PCs: (1) the diameter of the air holes is 210 nm; and the square lattice constant is $a = 320$ nm; (2) bulk refractive index of SiO_2: $n(SiO_2, \lambda_0) = 1.45$; (3) bulk refractive index of Si_3N_4: $n(Si_3N_4, \lambda_0) = 1.95$. The sub-diffractive propagation of TM- and TE-polarized beams takes place in the simulated sample at $\lambda_{TM} = 800$ nm and $\lambda_{TE} = 790$ nm, respectively [8].

Steeped grating of electric susceptibility, which represent holes, can be written in the following form: $\varepsilon(\mathbf{r}) = \bar{\varepsilon} + \Delta\varepsilon \sum_{l,m} \theta(|(l\mathbf{q}_1 + m\mathbf{q}_2) - \mathbf{r}| - |\mathbf{r}_0|)$, where $\Delta\varepsilon$ is the difference in the susceptibilities of the bulk material ($\bar{\varepsilon}$) and holes ($\bar{\varepsilon}_0 = 1$); indexes l and m numerate the position of the holes in a lattice, r_0 is the hole radius. We consider a structure with square symmetry, i.e. $|\mathbf{q}_1| = |\mathbf{q}_2|$, and when the reciprocal lattice vectors $\mathbf{q}_1$ and $\mathbf{q}_2$ are oriented at an angle $\alpha = 45°$ with respect to the direction of light propagation. As it has been shown previously in such PCs the sub-diffractive light propagation of stationary beams is possible along few directions [13]. Two of them are oriented at an angle $\alpha = 45°$ with respect to the reciprocal lattice vectors $\mathbf{q}_1$ and $\mathbf{q}_2$, and the other two directions are along $\alpha = 0°$. We consider the first directions, because, as it was shown [18] the spreading in the former case is slower than in the latter one.

Propagation of TM polarized waves (with electric field vector perpendicular to the plane of wave propagation) in 2D plane can be described by Maxwell's equations

$$\frac{\partial}{\partial t}\begin{pmatrix} B_x \\ B_z \\ D_y \end{pmatrix} = \begin{pmatrix} 0 & 0 & \partial_z \\ 0 & 0 & -\partial_x \\ \partial_z & -\partial_x & 0 \end{pmatrix}\begin{pmatrix} H_x \\ H_z \\ E_y \end{pmatrix}, \tag{1}$$

and for TE polarized waves (with magnetic field vector perpendicular to the plane of wave propagation), as described by Maxwell's equations

$$\frac{\partial}{\partial t}\begin{pmatrix} D_x \\ D_z \\ B_y \end{pmatrix} = \begin{pmatrix} 0 & 0 & -\partial_z \\ 0 & 0 & \partial_x \\ -\partial_z & \partial_x & 0 \end{pmatrix}\begin{pmatrix} E_x \\ E_z \\ H_y \end{pmatrix}, \tag{2}$$

where $E_\sigma(D_\sigma)$ are the components of electric field (displacement) vector, and $H_\rho(B_\rho)$ are the components of magnetic field (induction) vector, $\sigma = y$, $\rho = \{x, z\}$ are the indices of electric and magnetic field components; ∂_t and ∂_ρ denote the time and space derivatives, respectively. Modulation of electric susceptibility is accounted by the constitutive equations:

$$D_\sigma = E_\sigma \varepsilon_0 \varepsilon(\mathbf{r}), \quad B_\rho = H_\rho \mu_0. \tag{3}$$

Here we consider propagation of light pulses with central wavelengths near the one corresponding to non-diffractive regime reported previously, i.e. near $\lambda_{\text{TE}} - \lambda_{\text{TM}} = \lambda_0 = 800$ nm. First in order to determine the effective refractive index for 2D FDTD simulations of considered PC, we have calculated the effective refractive index of the planar guided modes in the $SiO_2/Si_3N_4/SiO_2$ waveguide without holes and we have found that it supports a single TE and a single TM polarized guided modes at $\lambda_0 = 800$. We have obtained the corresponding values for the effective refractive index of two guided modes: $n_{\text{TE}}(\lambda_0) = 1.748$ and $n_{\text{TM}}(\lambda_0) = 1.67$ for TE and for TM polarization, respectively. Next we integrated numerically the 2D problem with FDTD technique by using these values as the guide, and searched for the refractive index of the simulated PC material at which the sub-diffractive propagation takes place under the given 2D geometry of holes in the PC. We found that the most appropriate values for matching the experimentally observed sub-diffractive propagation are $n_{\text{TE}}(\lambda_0) = 1.7$ and $n_{\text{TM}}(\lambda_0) = 1.58$ for TE and for TM polarization, respectively. In the subsequent 2D FDTD simulations we used these values of refractive index. The values for the effective refractive index of the guided modes are slightly lower in the numerical simulation because the analytical values do not account for the filling factor associated with the holes. Therefore, we simulated TE/TM pulse propagation in 2D PC assuming that the PC material has refractive index $n_{\text{TE}}(\lambda_0) = 1.7 / n_{\text{TM}}(\lambda_0) = 1.58$ and the PC geometry (hole radius and lattice constant) is the same as in the real PC sample. The numerical simulations have been performed by FDTD method [20]. The spatial and time grid discretizations were $dx = dz = 20$ nm and $dt = 0.038$ fs, respectively. Calculations were performed on a grid size of which is $l_\perp = 16$ μm in transverse and $l_\parallel = 70$ μm in longitudinal direction. The spatial grid was terminated by the absorptive boundaries with uniaxial perfectly matched layers (UPML) [20]. For a given FDTD simulation we fixed the refractive index of the PC material (as described above) for waves with all frequencies, i.e. the dispersive properties of the PC material have not been taken into account. We assumed that the input pulses and beams have Gaussian profile in both transverse and longitudinal directions. Transverse width (double transverse waist) of the input pulses was $2w_\perp = 1.8$ μm. When temporal duration of pulses τ_P is considered as a control parameter it is varied in the range [10 fs, 40 fs]. When other parameters are considered as control ones the temporal pulse duration is fixed at 20 fs.

3. Analytical predictions

It is well known that diffraction length of electromagnetic waves (light) in homogeneous media is characterized by the Rayleigh length [1]

$$L_{\text{Rayleigh}}^{(\text{Homogeneous})} = n_{\text{eff}} \pi w_\perp^2 / \lambda_0, \tag{4}$$

where $w_\perp$ is the half width of the input beam.

Recently, it has been shown that in PCs the diffraction of stationary light beams can be described by the same parameter as the Rayleigh length but related to PC structure. For 2D planar PC with rhombic symmetry (which in particular cases can be reduced to the square and hexagonal types of symmetry) of the PC lattice such parameter for light propagated in the direction of symmetry axis can be written as follows:

$$L_{\text{Rayleigh}}^{(\text{PCs})} = n_{\text{eff}} \pi w_\perp^2 / (d_2 \lambda_0), \tag{5}$$

where coefficient d_2 is the leading order diffraction coefficient. The coefficient d_2 can be either positive (which means the normal diffraction), negative (which means anomalous diffraction) or equal to zero. The latter case corresponds to the sub-diffractive propagation of stationary light beams in PCs. In such a case the characteristic length $L_{\text{Rayleigh}}^{(\text{PCs})}$ becomes equal to infinity and the diffraction of the stationary light beams should be described by the high order diffraction coefficients. In particular, under the sub-diffractive regimes along symmetry direction of PCs with rhombic lattice (with square type of lattice among them) the next nonzero coefficient is of the fourth order d_4. For TM and TE polarized stationary light beams they have been obtained in Refs. [17,18]. The diffraction length in such a case (under sub-diffractive regime) can be written as follows [17]

$$L_{d4}^{(\text{PC})} = \pi^2 (q_\perp^2 + q_\parallel^2) w_\perp^4 / (4 d_4 \lambda_0), \tag{6}$$

where $q_{\perp(\parallel)} = 2\pi / \Lambda_{\perp(\parallel)}$ and $\Lambda_{\perp(\parallel)}$ is the period of refractive index modulation along (perpendicular) to the direction of beam propagation.

In Ref. [19] it has been shown that the diffraction of pulsed light beams in PCs could be described by the two diffraction–dispersion lengths. The first dispersion length given by the expression

$$L_{\text{PC},1} = \frac{2\pi c^2 \tau_P^2}{n_{\text{eff}} \lambda_0 W_i^{-1}} \frac{k_i^2}{(q_\perp^2 + q_\parallel^2)}, \tag{7}$$

depends on the initial pulse duration τ_P and it is responsible for the symmetric broadening of the pulse in time. It relates to the group velocity dispersion of PCs described by the parameter W_i^{-1} for TM or TE polarized waves, respectively ($i = $ TM, TE). k_i is the wavenumber for TM or TE polarized waves.

The second characteristic length is a mixed dispersion/diffraction length

$$L_{\text{PC},2} = w_\perp^2 2 k_i^2 c \tau_P / (n_{\text{eff}} \alpha_i), \tag{8}$$

that depends on the initial pulse duration τ_P and on the beam width $w_\perp$ at the input point. It results in a spatio-temporal broadening and asymmetric (in time) distortion of the pulse. This dispersion/diffraction length is an exceptional characteristic of PCs, since in homogeneous materials diffraction broadening and dispersive spreading is decoupled one from another.

In the expressions (5)–(8) the parameters are defined as follows

$$d_2^{(i)} = \left(\frac{8F_i^2}{(1-Q_{\|,i})^3}\frac{q_\|^2 a_i}{(q_\|^2+q_\perp^2)}-1\right), \quad a_{TM}=1,$$

$$a_{TE}=(1-q_\|/k_{TE})^2, \tag{9.a}$$

$$W_i^{-1}=\frac{Q_{\|,i}(4-3Q_{\|,i})}{4q_\perp^2/(q_\|^2+q_\perp^2)}b_i, \quad b_{TM}=1,$$

$$b_{TE}=\frac{\left(1-\frac{q_\perp^2/k_{TE}^2}{(4-3Q_{\|,TE})}\right)}{(1-q_\|/k_{TE})^2}, \tag{9.b}$$

$$\alpha_i=\frac{3Q_{\|,i}}{(1-Q_{\|,i})}+\frac{2\delta_{i,TE}}{(k_{TE}/q_\|-1)}, \tag{9.c}$$

$$F_i=\frac{fk_i^2}{(q_\|^2+q_\perp^2)}, \quad Q_{\|,i}=\frac{2k_iq_\|}{(q_\|^2+q_\perp^2)}, \quad f_i=\beta\delta\varepsilon_i/(4\varepsilon_i), \tag{9.d}$$

For 2D planar PCs with harmonic modulation of refractive index profile these coefficients have been obtained in Ref. [18] for TM polarized stationary light beams only. In this paper we generalize those expressions for both TM and TE polarized stationary light beams in the PCs with steeped profile of refractive index modulation by introducing in the parameter F a coefficient β that is a coefficient of the Heaviside function decomposition into the harmonics of refractive index modulation of considered PCs.

The values for the characteristics lengths in considered PC with effective refractive indexes $n_{TE}(\lambda_0)=1.7$ and $n_{TM}(\lambda_0)=1.58$ for TM and TE polarized light pulses with time duration of $\tau_P=20$ fs and pulse waist $w_\perp=0.9$ μm are presented in the Table 1. One can see that for both polarizations the diffraction spreading of the pulsed light beams is defined by the dispersion/diffraction length $L_{PC,2}$. But even for such short pulses, this diffraction length is larger than the Rayleigh length in the homogeneous media.

From the Table 1 it follows that the characteristic lengths of the pulsed beams in considered PC are larger for TE polarization than that for the TM case. Therefore, the TE polarized pulsed beams spread faster than that of the TM polarized ones.

Next we check the analytical predictions (7)–(9) by FDTD integration of 1,2. The numerical test is most spec-

tacular for extremely narrow beams (several μm), with, respectively short Rayleigh lengths (tens of μm). This is the most critical parameter range, therefore the analytical results (expressions (7)–(9)) as passing this range, should hold in the less parameter range of larger widths and, respectively longer propagation distances.

4. Numerical results

We calculated first the photonic band structure (Fig. 1) and the iso-frequency curves (Fig. 2) of the considered PC. The ZDP (straight segments of iso-frequency curves) in the first band occurs at normalized frequency of 0.40 (in units of a/λ) (see Fig. 2) which corresponds to the wavelength 800 nm. The considered PC has no complete photonic band gaps (PBG). In the ΓM direction, that is direction of sub-diffractive light propagation, there are pseudo-gaps between the frequencies of 0.434 and 0.455 (wavelength of 737.3 nm and 703.3 nm) for TE polarization (see Fig. 1a) and between frequencies of 0.445 and 0.474 (wavelength of 719 nm and 669.4 nm) for TM polarization (see Fig. 1b). Therefore, light beams with central wavelength of $\lambda_0=800$ nm are just below (in frequency) the band gap and therefore, they can propagate in the considered PC. Numerically we see the effects of the band gap for slightly lower region of wavelengths [see Fig. 6 (right column)] with respect to that obtained analytically.

Next we check numerically by FDTD integration of Eqs. (1 and 2) with Gaussian profile of the input pulse that sub-diffractive regimes take place close to the analytically defined wavelength. For this purpose transverse divergence of the pulses was analyzed by changing the light wavelength near $\lambda_0=800$ nm with other parameters of the PCs to be fixed. Profiles of the TE polarized pulses at propagation distance of 60 μm are presented in Fig. 3 at three different values of the central wavelength of the input pulse. We have found that by changing the central wavelength of the input pulse, the pulse propagation from the anomalous diffraction (see Fig. 3a–c) becomes sub-diffractive (see Fig. 3d–f) and then it becomes the normal one (see Fig. 3g–i). This figure also shows the changes in the temporal and transverse profile of the propagated pulses under changes of diffraction from anomalous and normal one through the sub-diffractive propagation. The same results (not presented here) have been obtained for the case of TM polarization.

Under sub-diffraction regimes the shape evolution of the TM- and TE polarized pulses at different propagation distances in the PC structure is presented in Figs. 4 and 5, respectively. In general we obtain an anticipated result that a pulse with initially Gaussian shape (both in transverse and longitudinal direction) distorts during the propagation through the PCs, and, in overall, it is broaden both in transverse and longitudinal direction. The distortion generally leads to the development of triangular shapes of the pulses (see Figs. 4 and 5). The distortion is hardly visible for pulse duration of 40 fs, but clearly visible for pulses

Table 1
Characteristic Lengths of propagated light beams

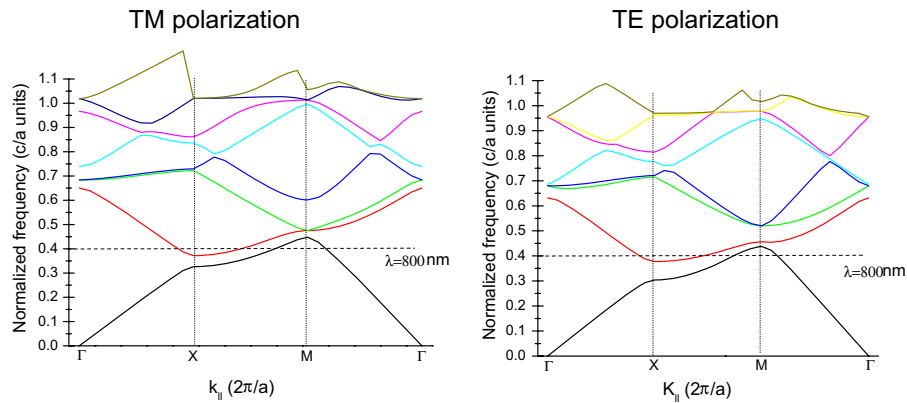| Light Polarization	$L_{\text{Rayleigh}}^{\text{(Homogeneous)}}$	$L_{PC,1}$	$L_{PC,2}$
TM	$6.25\lambda_0$	$244\lambda_0$	$47\lambda_0$
TE	$6.75\lambda_0$	$50\lambda_0$	$17\lambda_0$

Fig. 1. (Color online) Band structure of 2D PC with square lattice of air holes with a pitch of $a = 320$ nm and a hole diameter of $d = 210$ nm for TM (left) and TE (right) field polarization.
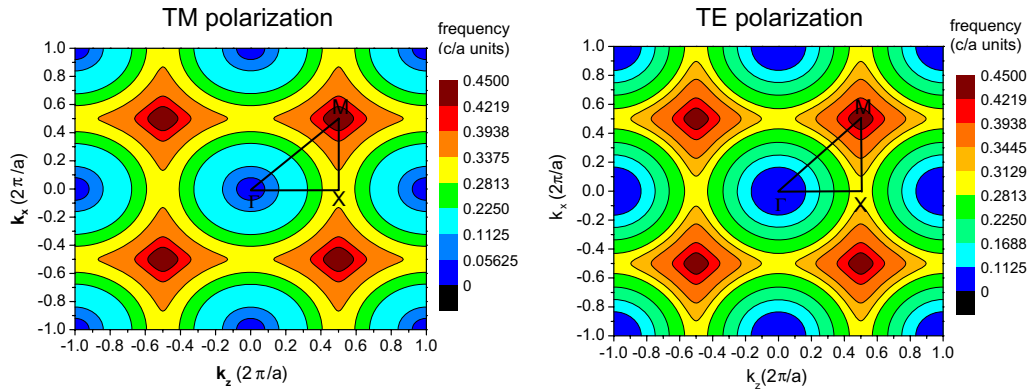

Fig. 2. (Color online) Iso-frequency curves of the first TM–like (left figure) and TE–like (right figure) band of the PC structure of Fig. 1.
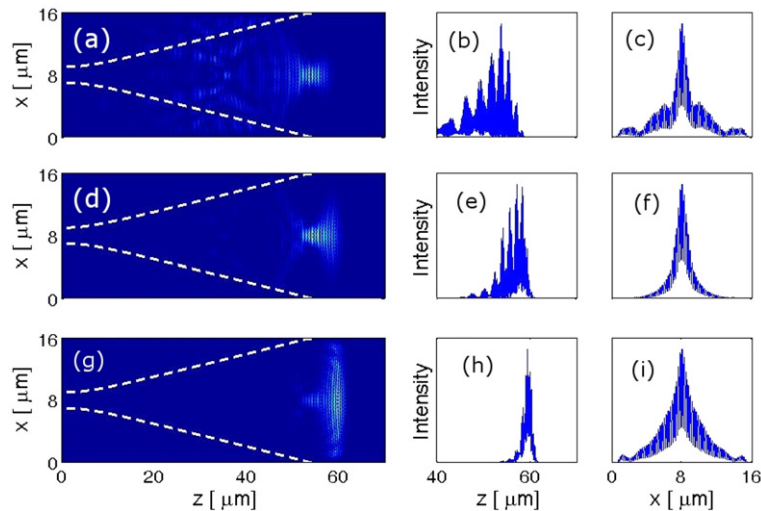

Fig. 3. (Color online) Spatial distribution of the electric field intensity (a, d, g), longitudinal (b, e, h) and transverse (c, f, i) profiles of TE polarized pulse at propagation distance $L_{\parallel} = 60$μm. The central wavelength of the input Gaussian pulses are $\lambda = 700$ nm (a–c), $\lambda = 790$ nm (d–f) and $\lambda = 900$ nm (g–i). The parameters are as follows: central wavelength of pulse $\lambda_0 = 800$ nm; effective index of refraction $n_{TE}(\lambda_0) = 1.70$; initial transverse width of the input Gaussian pulses is $2w_{\perp} = 1.8$ μm. Input pulse duration $\tau_P = 20$ fs. Dashed white lines in figures indicate spreading of pulse in homogeneous medium.
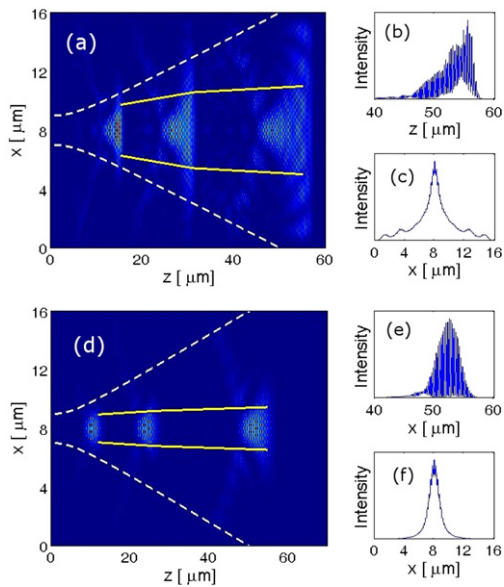
Fig. 4. (Color online) Spatial distribution of the electric field intensity and evolution of the transverse width at different propagation distances (a and d), longitudinal (b and e) and transverse (c and f) profiles of TM polarized pulse at propagation distance $L_{\parallel} = 60$ μm. Dashed (white) and solid (yellow) lines in figures indicate spreading of pulse in homogeneous medium and in considered PCs. The parameters are as follows: central wavelength of pulse $\lambda_0 = 800$ nm; effective index of refraction $n_{TM}(\lambda_0) = 1.58$; initial transverse width of the input Gaussian pulses is $2w_{\perp} = 1.8$ μm. Input pulse duration $\tau_P = 10$ fs (a) and $\tau_P = 40$ fs (b).
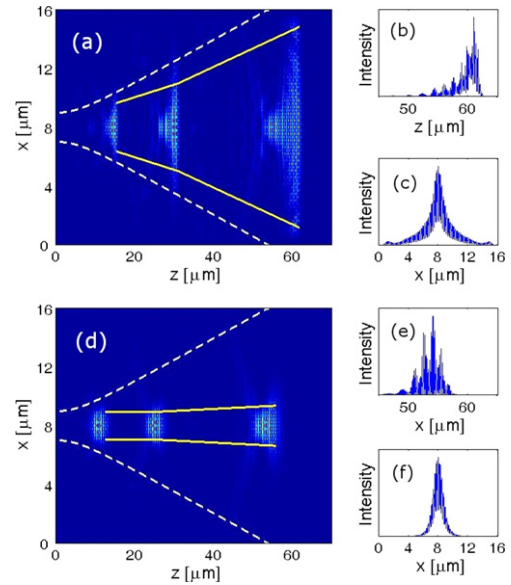

Fig. 5. (Color online) The same as in Fig. 4 but for TE polarized pulse. The parameters are the same as in Fig. 4 but with the effective index of refraction $n_{TE}(\lambda_0) = 1.70$.
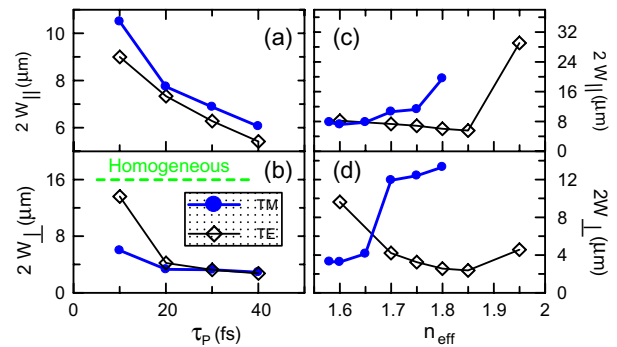

Fig. 6. (Color online) Dependence of pulse characteristics on the temporal duration (left column) and on effective refractive index of the guided modes (right column) for the input Gaussian pulse of TM (closed circles) and TE (open rhombuses) polarization. Pulse characteristics are calculated at propagation distance $L_{\parallel} = 60$ μm. To obtain the data for the left column the effective refractive index of the guided modes is fixed at $n_{TM} = 1.58$ for TM polarization and $n_{TE} = 1.70$ for TE polarization. For the right column the time duration of the input pulse is set to $\tau_P = 20$ fs. The other parameters of the input pulse and of the PC are the same as in Fig. 4 for TM polarization and as in Fig. 5 for TE polarization. The central frequency of the pulses is $\lambda_0 = 800$ nm. The natural dispersion of the material Si_3N_4 was neglected.

with duration less than 20 fs. It should be mentioned that the same form of the pulses has been reported previously in Ref. [19] under paraxial and slowly varying envelope approximations for TM polarized light in PCs with harmonic modulation of refractive index.

Moreover, from the plots presented in Figs. 4 and 5 one can also conclude that pulses of TE polarization diverge faster than TM polarized pulses, which stays in agreement with analytical predictions presented in the Table 1.

FDTD calculations have been performed for different temporal durations of the input Gaussian pulse. The results are summarized in Fig. 6a and b for both TM- and TE-polarized pulses. With increasing the temporal pulse duration the transverse pulse spreading decreases, i.e. the longer the pulse the slower its spreading in PCs. When the temporal duration of the input pulse approaches few optical circles, the spreading of the pulse in transverse direction becomes the same or even stronger than that in the homogeneous medium. This confirms analytical results presented in the previous section.

We have also investigated the dependence of the characteristics of the input Gaussian pulse with time duration of 20 fs on the effective refractive index of the waveguide modes as calculated after propagation distance of $L_{\parallel} = 60$ μm. The results for TM- and TE-polarized pulses are summarized in Fig. 6c and d and shown by closed circles and open rhombuses, respectively. One can conclude that the PC structure considered in this paper is optimum one for TM polarized pulses at the wavelength

$\lambda_0 = 800$ nm. But for TE polarization in order to decrease further the pulse spreading, the effective refractive index should be slightly increased.

In order to explore the persistence of sub-diffractive pulse propagation in large range of frequencies we investigated the dependence of the characteristics of the TE polarized pulse (with initial Gaussian profile and time duration of 20 fs) at propagation distance of $L_{\parallel} = 60$ μm on the central wavelength of the pulse. The results are plotted in Fig. 7. The data in this figure have been obtained for the
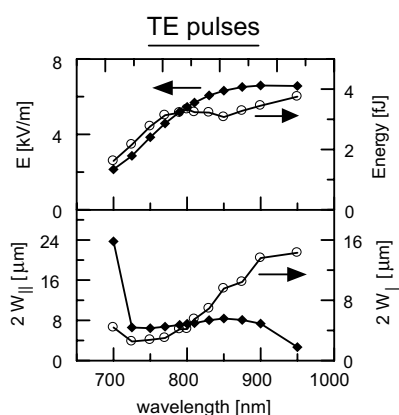
Fig. 7. Dependence of the pulse characteristics at propagation distance $L_\parallel = 60\ \mu m$ on the central wavelength of the input Gaussian pulse of TE polarization. The parameters are: $n_{TE} = 1.70$, $\tau_P = 20$ fs. The other parameters of the input pulse and of the PC are the same as in Fig. 5. Notation "E[kV/m]" means the maximum amplitude of the pulse envelope at considered propagation distance. The peak power of initial pulse in all simulations was 1 W, which corresponds to initial energy of 5 fJ for pulses with temporal duration of 20 fs.

PCs with effective refractive index for the guided TE modes as $n_{TE}(\lambda_0) = 1.70$. From this figure one can see that non-diffractive pulse propagation corresponds to the optimum value of the output pulse energy. Although the pulse width at propagation distance of $L_\parallel = 60\ \mu m$ could be smaller at central pulse wavelengths $\lambda < \lambda_0$, where the diffraction is anomalous one, but for this range of wavelength the losses of pulse energy during propagation is higher than for pulses propagated sub-diffractively at λ_0. Moreover, the transverse width of the pulses significantly increases at smaller wavelength because of the effects of the band gap, as well as for the pulses under normal diffraction condition, i.e. for pulses with central wavelength larger than that of the sub-diffractive regime. The same behavior (not shown in the Fig. 7) has been observed for the TM polarized pulses.

5. Conclusions

We conclude that the specific phenomena of sub-diffractive propagation of pulsed beams (PC induced spatial and temporal broadening, asymmetric spatiotemporal misshaping) as predicted theoretically in [19] can be observed on the existing samples [8], or on ones similar to those reported in Ref. [8], with steeped spatial profile of refractive index. The spatiotemporal broadening can be observed by recording full spatio-temporal pulse structure, however as well as by measuring the integral characteristics of the pulse: i.e. the integral width as obtained by integrating the intensity along the pulse, and the integral length, as obtained by integrating the intensity across the pulse. The

pulses as short as at least 40 fs are needed for the observation of the discussed effects, and the effects are strongly pronounced for the pulse durations less than 20 fs. Therefore, it has been theoretically shown for transfer and processing the data in the integrated micro and nanometer optoelectronic circuits, the sub-diffractive propagation regimes of light pulses with time duration larger than 20 fs can be feasible.

References

[1] M. Born, E. Wolf, Principles of Optics, Cambridge University Press, Cambridge, UK, 1999.
[2] H. Kosaka, T. Kawashima, A. Tomita, M. Notomi, T. Tamamura, T. Sato, Sh. Kawakami, Appl. Phys. Lett. 74 (1999) 1212.
[3] H.S. Eisenberg, Y. Silberberg, R. Marandotti, J.S. Aitchison, Phys. Rev. Lett. 85 (2000) 1863.
[4] T. Pertsch, T. Zentgraf, U. Peschel, A. Brauer, F. Lederer, Phys. Rev. Lett. 88 (2002) 093901.
[5] L. Wu, M. Mazilu, Th.F. Krauss, J. Light. Tech. 21 (2003) 561.
[6] D.W. Prather, Sh. Shi, D.M. Pustai, C. Chen, S. Venkataraman, A. Sharkawy, G.J. Schneider, J. Murakowski, Opt. Lett. 29 (2004) 50.
[7] R. Illiew, C. Etrich, U. Peschel, F. Lederer, M. Augustin, H.-J. Huchs, D. Schelle, E.-B. Kley, S. Nolte, A. Tunnermann, Appl. Phys. Lett. 85 (2004) 5854.
[8] M. Augustin, R. Iliew, C. Etrich, D. Schelle, H.-J. Huchs, U. Peschel, S. Nolte, E.-B. Kley, F. Lederer, A. Tunnermann, Appl. Phys. B 81 (2005) 313.
[9] Zh. Lu, Ch.A. Schuetz, Sh. Shi, C. Chen, G.P. Behrmann, D.W. Prather, IEEE Trans. Microwave Theory Tech. 53 (2005) 1362.
[10] Zh. Lu, Sh. Shi, J. Murakowski, G.J. Schneider, Ch.A. Schuetz, D.W. Prather, Phys. Rev. Lett. 96 (2006) 173902.
[11] J. Witzens, M. Loncar, A. Scherer, IEEE J. Selected Topics in Quantum Electron. 8 (2002) 1246.
[12] J. Witzens, A. Scherer, J. Opt. Soc. Am A. 20 (2003) 935.
[13] D.N. Chigrin, S. Enoch, C.M. Sotomayor Torres, G. Tayeb, Optics Express 11 (2003) 1203.
[14] S. Longhi, Phys. Rev. E 71 (2005) 016603.
[15] S. Longhi, D. Janner, Phys. Rev. B 70 (2004) 235123.
[16] K. Staliunas, Phys. Rev. Letts 91 (2003) 053901.
[17] K. Staliunas, R. Herrero, Phys. Rev. E 73 (2006) 016601.
[18] Yu. Loiko, C. Serrat, R. Herrero, K. Staliunas, Opt. Commun. 269 (2007) 128.
[19] K. Staliunas, C. Serrat, R. Herrero, C. Cojocaru, J. Trull, Phys. Rev. E 74 (2006) 016605.
[20] A. Taflove, S.C. Hagness, Computational Electrodynamics: The Finite-Difference Time-Domain Method, Artech House, Boston, 2000.